The Kinetics of Competing Multiple-Barrier Unimolecular Dissociations of *o*-, *m*-, and *p*-Chlorotoluene Radical Cations

Jongcheol Seo,[†] Hyun-Il Seo,[‡] Seung-Joon Kim,[‡] and Seung Koo Shin*,[†]

Department of Chemistry, Pohang University of Science and Technology, Pohang, Korea 790-784, and Department of Chemistry, Hannam University, Daejeon, Korea 300-791

Received: February 6, 2008; Revised Manuscript Received: May 17, 2008

The kinetics of competing multiple-barrier unimolecular dissociations of *o*-, *m*-, and *p*-chlorotoluene radical cations to $C_7H_7^+$ (benzyl and tropylium) are studied by ab initio/Rice−Ramsperger−Kassel−Marcus (RRKM) calculations. This system presents a very intriguing kinetic example in which the conventional approach assuming a single-barrier or a double-well potential surface with one transition state cannot predict or explain the outcome. The molecular parameters obtained at the SCF level of theory with the DZP basis set are utilized for the evaluation of microcanonical RRKM rate constants with no adjustable parameters. First-principles calculations provide the microscopic details of the reaction kinetics along the two competing multiple-barrier reaction pathways: the rate-energy curves for all elementary steps; temporal variations of the reactants, the reaction intermediates, and the products; and the product yield as a function of energy. The rate constant for each channel is calculated as a function of the internal energy at 0 K. After the thermal correction, the calculated rate-energy curves for the benzyl channel agree well with the photoelectron photoion coincidence data obtained at room temperature for all three isomers. Close agreement between experiments and theory suggests that first-principles calculations taking the full sequence of kinetic steps into account offer a useful kinetic model capable of correctly predicting the outcome of competing multiple-barrier reactions. The slowest process is identified as [1,2] and [1,3] α-H migration at the entrance to the tropylium and benzyl channel, respectively. However, the overall rate is determined not by the slowest process, but by the combination of the slowest rate and the net flux toward the product, which is multiplicatively reduced with an increasing number of reaction intermediates. The product yield calculation confirms the benzyl cation as the predominant product. For all isomers, the thermodynamically most stable tropylium ion is produced much less than expected because a large fraction of flux coming into the tropylium channel goes back to the benzyl channel. The benzyl channel is kinetically favored because it involves a lower entrance barrier with fewer rearrangements than the tropylium channel.

Introduction

The mechanism of the formation of $C_7H_7^+$ from unimolecular dissociations of halotoluene radical cations has attracted much interest in experiment[1–16] and theory[17–19] because it involves complicated rearrangement processes to the benzyl cation, the tropylium ion, or both, with loss of a halogen atom or direct C−X (X: halogen) cleavage to the tolyl cation. The direct cleavage channel competes with rearrangement in iodotoluene radical cations, in which the C−I bond is relatively weak.[4,8–12] For bromo- and iodotoluene radical cations, the rate of energy-selective dissociation was determined from experiments employing photoelectron−photoion coincidence (PEPICO) spectroscopy[7] and time-resolved photodissociation (TRPD) spectroscopy.[14,15] The structure of $C_7H_7^+$ from TRPD was identified as the benzyl cation from ion cyclotron resonance (ICR) experiments monitoring ion−molecule reactions of $C_7H_7^+$ with toluene-d_8.[14–16] For chlorotoluene radical cations, the rate was derived from PEPICO experiments,[7] but the structure of $C_7H_7^+$ from energy-selective dissociation was not firmly established. Collisional activation (CA) studies claimed a mixture of both the benzyl and tropylium ions as the products from unimolecular dissociations of chlorotoluene radical cations,[7] but recent product-resolved studies of the energy-selective dissociation of bromo- and iodotoluene radical cations has suggested the benzyl cation as the lowest barrier product.[14–16] Unfortunately, time- and product-resolved photodissociation experiments could not be performed with chlorotoluene radical cations because they lack absorption in the wavelength range of 475−575 nm.

To identify the minimum energy reaction pathways to both the benzyl and tropylium ions from *o*-, *m*-, and *p*-clorotoluene radical cations, our group carried out ab initio calculations and reported the structures and relative energies of the local minima and the transition states along the dissociation pathways.[19] Figure 1 shows the reaction pathways considered in ab initio calculations and the energy levels of the local minima, the transition states, and the products relative to the reactants obtained at the SCF level of theory with the DZP basis set.[19] Figure 2 illustrates the structures of the reactants, the reaction intermediates, and the products depicted in Figure 1. Formation of the benzyl cation involves a series of rearrangement processes prior to C−Cl cleavage: [1,3] sigmatropic migration of an α-H atom to the ortho position at the entrance, which is common to all three isomers, followed by [1,2] H-atom migration on a six-membered ring for *m*- and *p*-isomers. Formation of the tropylium ion involves more than H-atom migration: The first step, common to all three isomers, is [1,2] sigmatropic migration of an α-H atom to the ipso position at the entrance, and subsequent steps

* Corresponding author. E-mail: skshin@postech.ac.kr.
[†] Pohang University of Science and Technology.
[‡] Hannam University.

10.1021/jp801098p CCC: $40.75
Published on Web 07/02/2008

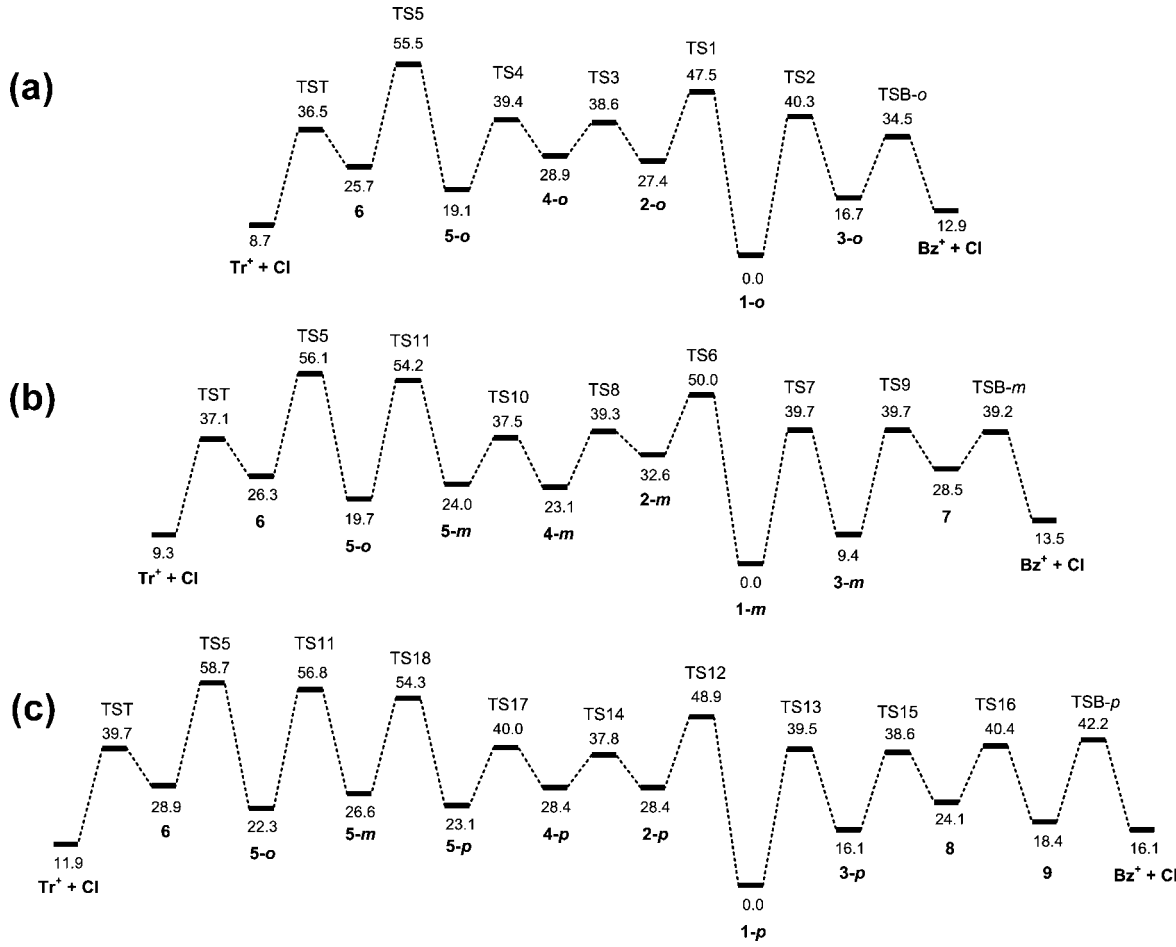

Figure 1. The minimum energy path to $C_7H_7^+$ (benzyl and tropylium) from (a) the *o*-chlorotoluene radical cation (**1**-***o***), (b) the *m*-isomer (**1**-***m***), and (c) the *p*-isomer (**1**-***p***). The nomenclatures are adopted from Kim et al.[19] The energy levels are relative to the reactants, **1**-***o***, **1**-***m***, and **1**-***p***, for each isomer. Energies are given in units of kcal mol^{-1}.

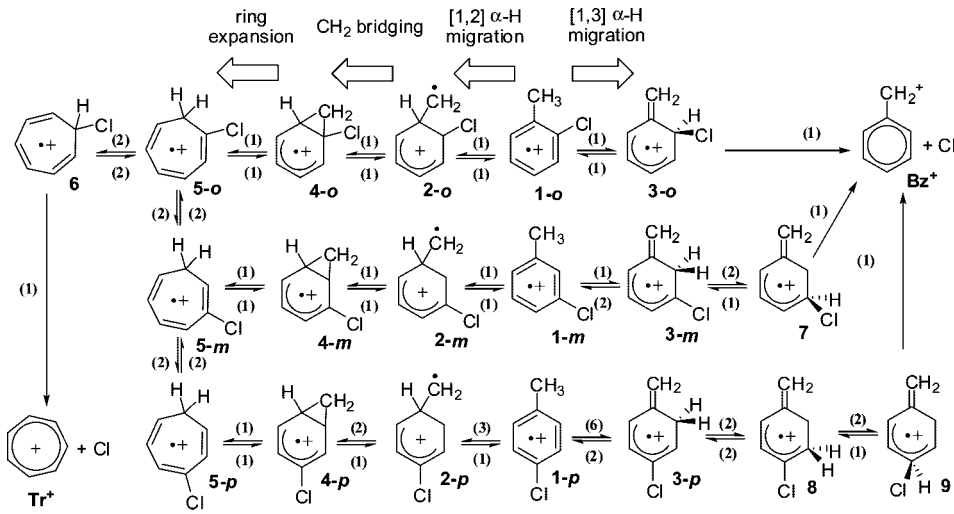

Figure 2. The mechanism of unimolecular dissociation of *o*-, *m*-, and *p*-chlorotoluene radical cations. The value in parentheses represents the reaction degeneracy for each elementary step.

involve [1,2] CH_2 migration to form a methylene bridge, followed by ring expansion as well as [1,2] H-atom migration on a seven-membered ring to form cycloheptatrienyl chloride prior to C−Cl cleavage. Thus, this system presents a very intriguing kinetic example in which the two reactions compete with each other on a multiple-barrier potential energy surface so that the overall kinetics are neither predictable nor explicable within a conventional framework assuming a single-barrier or a double-well potential surface with one transition state.

Although ab initio calculations identify the minimum energy pathways involving a series of consecutive rearrangement processes to the two competing product channels, the barrier heights and thermodynamic stabilities alone do not tell us the detailed kinetics: how the two channels compete with one another, what determines the overall reaction rate, and how the reaction rate and the product yield vary with internal energy. To get a useful kinetic model correctly describing the competing multiple-barrier reactions, we have to simulate the full sequence

of kinetic steps based on first principles. To this end, we carried out Rice−Ramsperger−Kassel−Marcus (RRKM) calculations[20] based on the ab initio molecular parameters.[19] The statistical theory, such as RRKM, is well-suited for this problem because the intramolecular vibrational relaxation occurs faster than the rearrangement or dissociation processes for medium-sized molecules, such as chlorotoluene, and all rearrangement or dissociation steps involve distinct transition states with well-defined reverse barriers. Ab initio/RRKM calculations allow the evaluation of the microcanonical dissociation rate constants from first principles with no adjustable parameters. Thus, the controversies over the mechanisms of the formation of $C_7H_7^+$ (benzyl vs tropylium) can be resolved without a priori assumptions.

We simulated the kinetics of unimolecular dissociations and evaluated thermodynamic parameters for activation. First, we obtained the entropy of activation to see the tightness of the transition states as well as the enthalpy and Gibbs free energy of activation. We then calculated the RRKM rate constants for all forward and reverse reactions involved in the dissociation pathways as a function of internal energy at 0 K and derived the rate constant for each channel. To compare theoretical results with the PEPICO data obtained at 298 K,[7] the RRKM rate constants were corrected for thermal energy. After the thermal correction, the RRKM rate-energy curves for the benzyl channel are in excellent agreement with the PEPICO data for all three isomers. First-principles calculations not only confirm the recent experimental findings of Kim and Shin[14–16] but also corroborate the proposed dissociation mechanisms. Finally, we examined temporal variations of all reaction intermediates to see how the reaction propagates in time and calculated the product yield numerically by taking both channels into account.

Calculational Detail. Ab initio calculations for the geometries and relative energies of the local minima and the transition states along the dissociation pathways of chlorotoluene radical cations have been described in detail elsewhere.[19] Molecular parameters, such as the vibrational frequencies and the rotational constants for all transient species, are given in Tables S1 and S2 (see the Supporting Information). All vibrational frequencies are round off to the nearest integer values to directly count the density and sum of vibrational states in a 1-cm^{-1} interval.

Thermodynamic parameters for the reaction, such as the entropy, enthalpy, and Gibbs free energy of activation, were calculated from the canonical partition function. The entropy of activation $\Delta S_T^{\ddagger}$, which describes the tightness of transition state, was evaluated using eq 1.[21]

$$\Delta S_T^{\ddagger} = k_B \frac{d}{dT}\left(T \ln \frac{Q^{\ddagger}}{Q}\right) \quad (1)$$

Q and $Q^{\ddagger}$ are the canonical partition functions for the reactant and the transition state, respectively, and they are evaluated from vibrational frequencies, rotational constants, and molecular mass. The enthalpy of activation $\Delta H_T^{\ddagger}$ was evaluated from the difference in energy and heat capacity between the reactant and the transition state. The heat capacity was derived from the canonical partition function. The Gibbs free energy of activation $\Delta G_T^{\ddagger}$ was calculated from the enthalpy and entropy of activation.

The RRKM calculation was carried out by using a homemade program. The RRKM rate constant for a unimolecular reaction is given by eq 2.[20]

$$k(E) = \frac{\sigma W^{\ddagger}(E - E_0 - E_r^{\ddagger})}{h\rho(E - E_r)} \quad (2)$$

σ is the reaction degeneracy, E is the internal energy of an ion, and E_0 is the energy of a critical activated configuration relative to the reactant corrected for the zero-point vibrational energy. E_r and $E_r^{\ddagger}$ represent the adiabatic rotational energies of the reactant and the activated configuration. $W^{\ddagger}(E - E_0 - E_r^{\ddagger})$ is the sum of vibrational states in the activated configuration over the internal energy from 0 to $E - E_0 - E_r^{\ddagger}$, and $\rho(E - E_r)$ is the density of vibrational states of the reactant at the internal vibrational energy $E - E_r$. Theoretically determined transition states were taken as critical activated configurations. The sum and density of states were calculated using a Beyer−Swinehart direct counting algorithm.[20] Each normal mode of vibration was treated as a harmonic oscillator. The internal rotation of the methyl group was also treated as a harmonic oscillator. Because all of the rearrangement processes take place around the planar ring, the angular momentum along the axis perpendicular to the ring plane was assumed to be conserved. As a result, the rotation with the highest moment of inertia was treated adiabatically, whereas the other two rotations were considered to be mixed with vibrational modes. The energy for the adiabatic rotation, E_r or $E_r^{\ddagger}$, was subtracted from the available internal energy.

The rate constants for the forward and reverse reactions in all elementary steps shown in Figure 2 were calculated at both 0 and 298 K in the energy range of 15 000−42 000 cm^{-1} at every 1 cm^{-1} step. For the rate constants at 298 K, we took thermal energy into account by setting $E_r = k_B T/2$ corresponding to one adiabatic rotation. To determine the overall dissociation rate, we simulated the reaction kinetics at both 0 and 298 K by setting up a matrix equation for each channel from a set of linear first-order differential equations (see the Supporting Information for details). The rate-constant matrix was filled with the microcanonical RRKM rate constants evaluated at each internal energy. The MATLAB program was used to solve the matrix equation and simulate the reaction kinetics. The populations of the reactant and reaction intermediates were calculated numerically at every 10^i ns ($i = 0-3$ for the benzyl channel and 1−4 for the tropylium channel) until the total number of temporal points reached 10 000. The product population was obtained for each channel by subtracting the sum of the populations of the reactant and reaction intermediates from the initial reactant population. The overall microcanonical dissociation rate constant, $k_{uni}(E_v)$, was determined by fitting the depletion of the sum of reactant and reaction intermediates to a single exponential function in the internal energy range of 15 000−42 000 cm^{-1} for each channel at every 200 cm^{-1} step.

To compare the calculated rate constant with the PEPICO data obtained at 298 K, we integrated $k_{uni}(E + E_v)$ over the Boltzmann distribution of the vibrational energy, E_v, of the reactant as given in eqs 3−5. The IR radiative relaxation of an energized molecule was not considered in the kinetic modeling.

$$k_T(E) = \int_0^{\infty} k_{uni}(E + E_v)\, P(E_v)\, dE_v \quad (3)$$

$$P(E_v) = \frac{\rho(E_v)\exp(-E_v/k_B T)}{Q_v} \quad (4)$$

$$Q_v = \sum \rho(E_v)\exp(-E_v/k_B T) \quad (5)$$

$P(E_v)$ is the probability of finding a vibrational level at the energy E_v, and Q_v is the canonical particion function resulting from the vibrational degrees of freedom.

For the calculation of the product yield, however, the reactant was allowed to branch out and cross over to both channels. The product yield was calculated in the internal energy range of 21 000−40 000 cm^{-1} at 298 K by numerically tracing the reaction until the product population (the sum of benzyl and

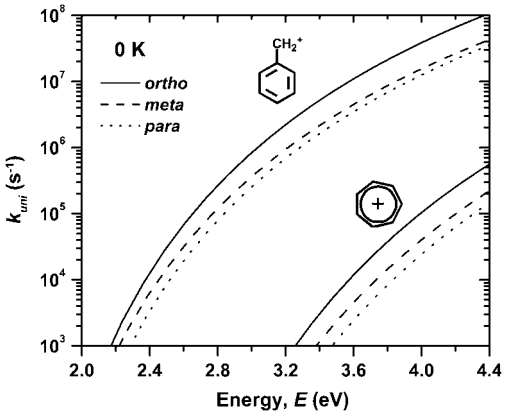

Figure 3. The RRKM rate constants at 0 K for the benzyl and tropylium channels.

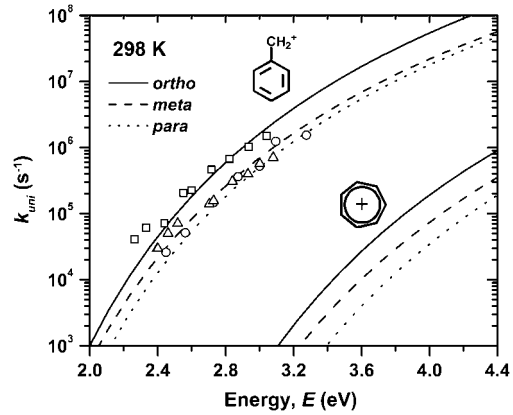

Figure 4. The RRKM rate constants at 298 K for benzyl and tropylium channels. The PIPECO data were taken from Olesik et al.:[7] the *o*-isomer (open square), the *m*-isomer (open circle), and the *p*-isomer (open triangle).

tropylium ions) reached 99%. To visualize the kinetics of the two competing parallel reactions, we examined temporal variations of the reactant, reaction intermediates, and the two products at 298 K with an internal energy of 25 000 cm^{-1} by tracing the populations every 0.1 ns for 4 μs.

Results

Thermodynamic parameters for the activation ($\Delta S^{\ddagger}_{298}$, $\Delta H^{\ddagger}_{298}$, $\Delta G^{\ddagger}_{298}$) evaluated at 298 K are summarized in Table S3 (see the Supporting Information). Between the two channels, $\Delta S^{\ddagger}_{298}$ for [1,2] α-H migration toward the tropylium channel is 0.8 ± 0.3 cal mol^{-1} K^{-1} more negative than $\Delta S^{\ddagger}_{298}$ for [1,3] α-H migration toward the benzyl channel for all three isomers, suggesting a more tight entropic bottleneck toward the tropylium channel. The *p*-isomer has more negative entropy of activation for α-H migration than the *o*- or *m*-isomer because of the reduction in molecular symmetry. Of the elementary steps, the CH_2 bridging process forming a bicyclic intermediate **4-*x*** from **2-*x*** ($x = o, m, p$) in the tropylium channel has the most negative entropy of activation with a value of −5.5 ± 0.6 cal mol^{-1} K^{-1}. In contrast, the ring expansion process forming a seven-membered ring **5-*x*** from **4-*x*** ($x = o, m, p$) in the tropylium channel has $\Delta S^{\ddagger}_{298}$ of only −0.6 ± 0.2 cal mol^{-1} K^{-1}. On the other hand, C−Cl cleavage involves $\Delta S^{\ddagger}_{298}$ in the range of −0.8 to +0.2 cal mol^{-1} K^{-1} for all three isomers, indicating that the transition state is neither so tight nor loose.

Figure 3 shows the rate-energy curves obtained at 0 K in the energy range of 2.0−4.4 eV. The overall rates of dissociation to both the benzyl and tropylium channels decrease in order, ortho > meta > para. The dissociation rate of the benzyl channel is at least 3 orders of magnitude greater than that of the tropylium channel for all three isomers. In the benzyl channel, the *o*-isomer dissociates 2−3 times faster than the other two isomers, and the *m*-isomer dissociates slightly faster than the *p*-isomer. However, the slope varies with isomer: With increasing energy, the *o*-isomer becomes increasingly faster than the other two isomers, and the *p*-isomer catches up with the *m*-isomer at high energy. In the tropylium channel, the *o*-isomer dissociates ∼2 times faster than the *m*-isomer, which again dissociates ∼2 times faster than the *p*-isomer. The slope varies with isomer similarly to the benzyl channel. It is noteworthy to mention here that, in the case of the *p*-isomer, the 3-fold rotational symmetry of the methyl group is considered in counting the reaction degeneracy of the reaction pathways shown in Figure 2. SCF calculations with the DZP basis set yielded an internal rotational barrier of 1.66, 1.05, and 0.0 kcal mol^{-1}, after zero-point energy correction, for the methyl group in the *o*-, *m*-, and *p*-isomer, respectively. Because the thermal energy of a 1-D internal rotor is $k_BT/2 = 0.30$ kcal mol^{-1} at 298 K, the methyl group in the *p*-isomer is considered a free rotor, whereas those in the other two isomers are considered hindered rotors. Thus, the reaction degeneracy of [1,3] and [1,2] α-H migration for the *p*-isomer is 6 and 3, respectively, whereas those for the *o*- and *m*-isomers are 1.

Figure 4 shows the rate constants as a function of internal energy corrected for thermal contributions at 298 K, along with the PEPICO data.[7] The thermal correction shifts the rate-energy curves to a lower energy side. The PEPICO data fall closely on the rate-energy curves for the benzyl channel in all three isomers. Thus first-principles calculations confirm that the lowest barrier rearrangement pathway leads to the benzyl cation, corroborating the recent experimental findings of Kim and Shin.[14–16]

To see what determines the overall reaction rate, we examined the rate-energy curves for all elementary reactions involved in the reaction pathways. Figures 5 and 6 show the rate-energy curves for the benzyl and tropylium channel, respectively, in the internal energy range of 2.5−5.0 eV. As expected, the rates of elementary reactions at low energy are primarily determined by the barrier height. The entropy of activation becomes the key factor determining the slope with increasing energy. When barrier heights are comparable, the rates are governed by the entropy of activation and the reaction degeneracy.

In the benzyl channel, the slowest process is [1,3] α-H migration (**1-*x*** → **3-*x***) which has the highest barrier. The rate for **1-*x*** → **3-*x*** is comparable to one another, but ascends in order ortho < meta < para. In contrast, the overall reaction rate descends in order ortho > meta > para, suggesting that the overall rate is not determined by the slowest process alone. The reaction mechanisms of the benzyl channel consist of the two-, three-, and four-step processes involving 1, 2, and 3 reaction intermediates for the *o*-, *m*-, and *p*-isomers, respectively, as shown in Figure 1. In the case of the *o*-isomer with only 1 intermediate, the first equilibrium greatly favors **1-*o*** over **3-*o***, and subsequent C−Cl cleavage from **3-*o*** occurs much faster than equilibrium. For the *m*-isomer with 2 intermediates, the first equilibrium favoring **1-*m*** over **3-*m*** proceeds more slowly than the second equilibrium favoring **3-*m*** over **7**, and final C−Cl cleavage from **7** occurs faster than the two preceding equilibria. For the *p*-isomer with 3 intermediates, the first and second equilibria prefer for **1-*p*** over **3-*p*** and **3-*p*** over **8**, respectively; the third equilibrium favors **9** over **8**; and the final C−Cl cleavage from **9** occurs with almost the second slowest rate.

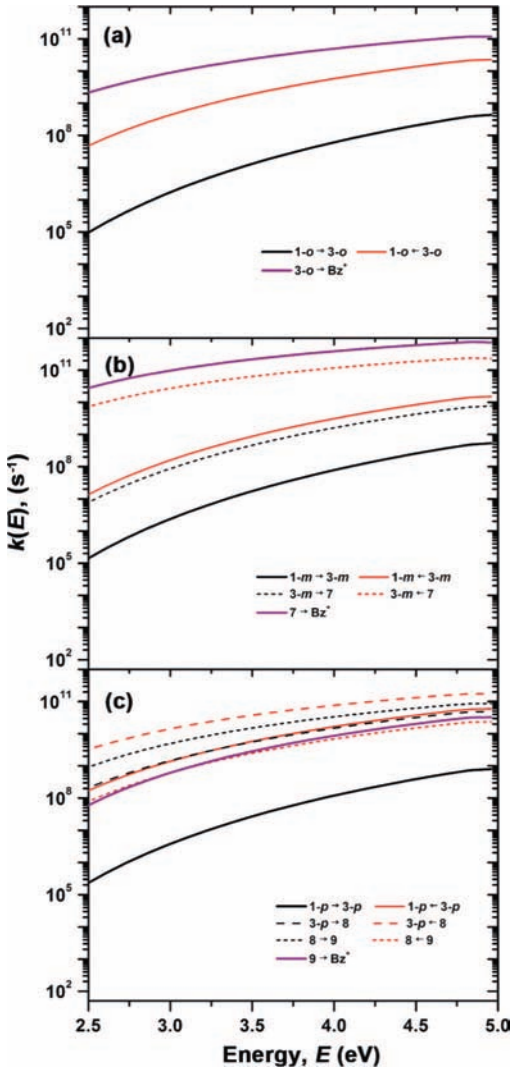

Figure 5. RRKM rate−energy curves for all elementary steps of the benzyl channel for (a) *o*-, (b) *m*-, and (c) *p*-chlorotoluene radical cations at 298 K.

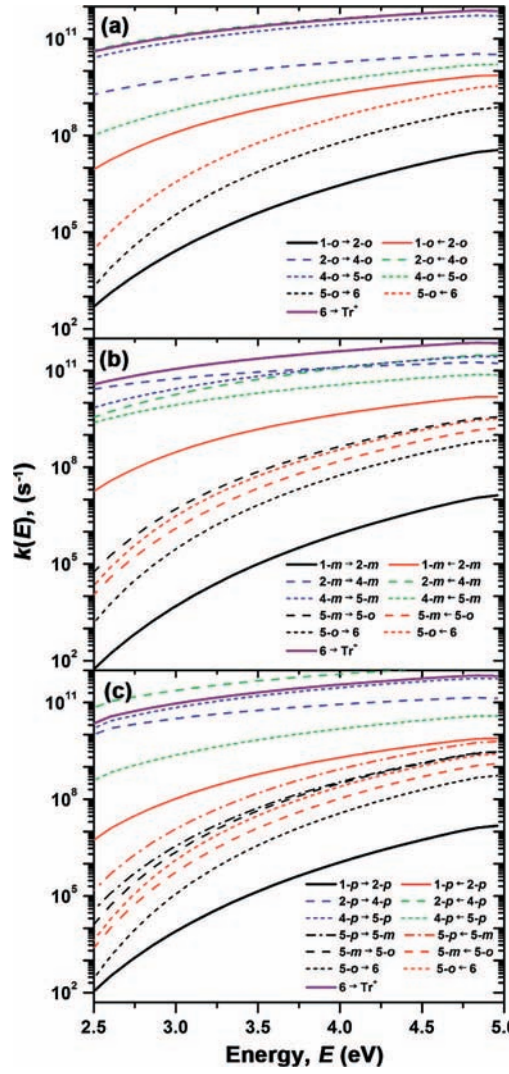

Figure 6. RRKM rate−energy curves for all elementary steps of the tropylium channel for (a) *o*-, (b) *m*-, and (c) *p*-chlorotoluene radical cations at 298 K.

Thus, the overall rate is determined by a combination of the rate of the slowest process **1**-***x*** → **3**-***x*** and the net flux toward Bz^+ from **3**-***x***, which is multiplicatively reduced with an increasing number of reaction intermediates.

In the tropylium channel, [1,2] α-H migration (**1**-***x*** → **2**-***x***) having the highest barrier is the slowest process, and [1,2] hydrogen migration from **5**-***o*** to **6** with the second-highest barrier is the second-slowest process. The rate for **1**-***x*** → **2**-***x*** descends in order ortho > para > meta. The order of meta and para is switched from the descending order of the overall reaction rate, ortho > meta > para. The tropylium channel consists of the five-, six-, and seven-step processes involving 4, 5, and 6 reaction intermediates for the *o*-, *m*-, and *p*-isomers, respectively. The reactant undergoes a series of rearrangements before it reaches a common intermediate, **5**-***o***, which leads to the tropylium ion Tr^+ via **6**. Both forward and backward H-atom migration between **5**-***o*** and **6** are slow, but final C−Cl cleavage from **6** is extremely fast. Thus, once arriving at **6**, the reaction would yield Tr^+. So the overall rate represents the rate of the appearance of **6**. For all three isomers, the slow first equilibrium favors **1**-***x*** over **2**-***x***, but fast second and third equilibria drive the reaction toward **5**-***x***. Therefore, the overall rate is determined by the combination of the rate of the slowest process **1**-***x*** → **2**-***x*** and the net flux from **5**-***x*** to **6**.

To identify kinetically important reaction intermediates in the reaction mechanisms, we combined both channels and examined temporal variations of the reactant, the reaction intermediates, and the products involved in the two competing reaction pathways. Figure 7 shows semilogarithmic plots of the temporal variations of all chemical species involved in both channels at an internal energy of 3.1 eV. The reactant disappears at the rate descending in order ortho > meta > para. The relative abundances of reaction intermediates vary with isomer: For ortho (Figure 7a), **5**-***o*** is the most abundant, although its precursor **4**-***o*** is not visible on this scale. The relative abundances of **2**-***o*** and **3**-***o*** become comparable with one another after an induction period. For meta (Figure 7b), **3**-***m*** is the most abundant and **5**-***o*** becomes second after an induction period. For para (Figure 7c), **3**-***p*** and **9** are the most and second-most abundant, respectively, whereas **5**-***o*** becomes third after an induction period. The tropylium ion reaches a maximum yield of <0.03%, which descends in the order ortho > meta > para. For all isomers, the tropylium ion yield is much less than expected from the integration of **5**-***o***, indicating that a large fraction of flux coming into the tropylium channel goes back to the benzyl channel. Thus, the reactant **1**-***x*** ($x = o, m, p$) is mostly depleted through the benzyl channel, thereby inducing all reaction

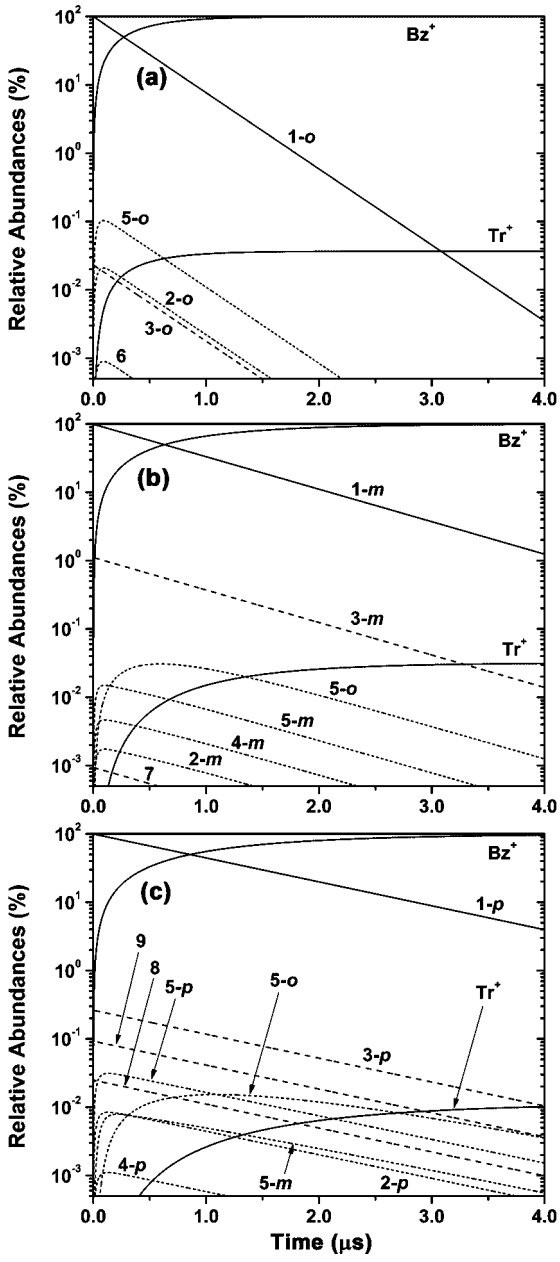

Figure 7. Temporal variations of the reactants, the products, and the reaction intermediates along the dissociation pathways to $C_7H_7^+$ for (a) *o*- (b) *m*-, and (c) *p*-chlorotoluene radical cations with an internal energy of 3.1 eV at 298 K. Solid lines denote the reactants and the final products. Long and short dashes represent the reaction intermediates involved in the benzyl and tropylium channels, respectively.

intermediates in both channels to decay at almost the same rate as the reactant **1**-*x*.

Finally, the relative yield of the products is shown in Figure 8 as a function of internal energy. The tropylium ion yield increases with increasing energy but remains less than ~1%, even at 4.8 eV. The *o*-isomer yields the tropylium ion most. The tropylium ion yield of the *m*-isomer is almost identical to that of the *o*-isomer, whereas that of the *p*-isomer is less than the other two isomers. Evidently, the tropylium channel is simply no competition to the benzyl channel in all isomers.

Discussion

Although the tropylium ion is thermodynamically more stable than the benzyl cation, the benzyl channel is much more

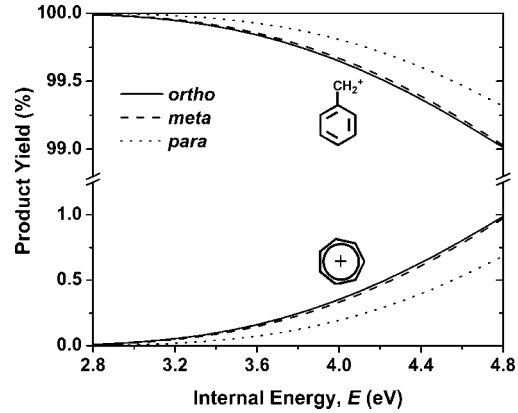

Figure 8. The calculated product yield for the benzyl and tropylium ions at 298 K.

kinetically accessible because the benzyl channel involves three fewer reaction intermediates for all three isomers and consists of only H-atom migration on the way to C−Cl cleavage, rather than the combination of H-atom migration, CH_2 bridging, ring expansion, and H-atom migration on a seven-membered ring.

In our previous analysis of the experimental rate-energy data for halotoluene radical cations with RRKM theory, we assumed a single-barrier potential surface consisting of a reactant and a critical activated configuration and treated vibrational frequencies and the activation energy as adjustable parameters.[4–16] From the best-fit parameters, we derived the activation energy and the entropy of activation and discussed the difference in barrier height and tightness of the transition state among isomers. The present ab initio/RRKM approach clearly manifests that both the activation energy and the entropy of activation are not well-defined parameters in a multiple-barrier system having no specific single rate-determining step. For instance, we previously thought that the *o*-isomer's dissociating faster than the other two isomers in halotoluene radical cations should have a lower activation energy, thus invoking the resonance effect of ortho halogen donating electrons for the stabilization of the transition states for α-H migration.[15,16] To the contrary, the calculated barrier height for [1,3] α-H migration toward the benzyl channel is almost comparable to one another, 40.3, 39.7, and 39.5 kcal mol^{-1} for the *o*-, *m*-, and *p*-isomer, respectively, showing no resonance effect on the stabilization of the transition states. In comparison, [1,2] α-H migration toward the tropylium channel with barrier heights of 47.5, 50.0, and 48.9 kcal mol^{-1} for the *o*-, *m*-, and *p*-isomers, respectively, shows some resonance effects of halogen stabilizing ortho and para more than meta. First-principles calculations clearly show that the *o*-isomer dissociates faster than the other two isomers, not because of the difference in barrier height of the slowest processes, but because it involves fewer reaction intermediates prior to the final C−Cl cleavage. As the number of reaction intermediates increases in going from ortho to meta and to para, each additional reaction intermediate reduces the net flux toward the product because the total outgoing flux from the reaction intermediate is branched out into both the forward and backward directions. We also thought that the entropy of activation derived from the experimental rate−energy curves from one halotoluene system was transferable to other halotoluene systems, thereby reducing the adjustable parameters for kinetic modeling,[11,13–16] but that assumption is turned out to be groundless, after all. The present approach with no a priori assumptions suggests that the mechanism is transferable from one system to another, but not the entropy of activation because the overall rate is not determined by any single process.

Last, the present results shed light on the reaction mechanisms. Interestingly, the transition states are grouped together in energy by their modes of activation for all three isomers. All the transition states for hydrogen migration in the benzyl channel lie at almost the same energy levels, within 39.4 ± 1.0 kcal mol^{-1} above the reactants. In the tropylium channel, those for [1,2] α-H migration lie within 48.8 ± 1.3 kcal mol^{-1}; those for both CH_2 bridging and ring expansion, within 38.8 ± 1.2 kcal mol^{-1}; and those for hydrogen migration on a seven-membered ring, within 55.5 ± 1.3 kcal mol^{-1}. The fact that hydrogen migration on a seven-membered ring is a higher barrier process than both CH_2 migration and bridging leads us to propose alternate pathways for the *m*- and *p*-isomers in the tropylium channel. By taking **4**-***m*** ⇌ **2**-***o***, the *m*-isomer could arrive at **5**-***o*** without going through the higher barrier process **5**-***m*** ⇌ **5**-***o***. Similarly, by taking **4**-***p*** ⇌ **2**-***m*** ⇌ **4**-***m*** ⇌ **2**-***o***, the *p*-isomer could bypass two consecutive higher barrier processes, **5**-***p*** ⇌ **5**-***m*** ⇌ **5**-***o***. Although these alternate routes involve one more intermediate than the mechanisms presented in this work, they are considered viable because both CH_2 migration and bridging are so rapid as compared with hydrogen migration on a cycloheptatrienyl chloride radical cation. So the maximum rate for the *m*- and *p*-isomers in the tropylium channel could approach the rate of the *o*-isomer. Nevertheless, the tropylium channel is considered no match for the benzyl channel.

Conclusions

The controversies over the mechanisms of the formation of $C_7H_7^+$ (benzyl vs tropylium) from unimolecular dissociations of halotoluene radical cations are finally resolved. A close agreement between the theoretical rate−energy curves for the benzyl channel calculated from first principles and the PEPICO experimental data in all three isomers substantiates the mechanisms which consider the hydrogen atom as an active species migrating along the reaction pathways. Ab initio/RRKM calculations validate the benzyl cation as the predominant product. Although the tropylium ion is thermodynamically more stable than the benzyl cation, the benzyl channel is kinetically much more accessible than the tropylium channel for all three isomers because it involves three fewer reaction intermediates with a lower entrance barrier and consists of only H-atom migration on the way to C−Cl cleavage rather than a complex combination of multiple skeletal rearrangements. First-principles calculations also show that no single step determines the overall rate in a multiple-barrier process. Thus, both the activation energy and the entropy of activation defined in a single-barrier process are not well-defined parameters for the multiple-barrier process.

Acknowledgment. S.-J. Kim acknowledges support from Hannam University in 2007. This work was supported by the Korea Research Foundation (Grant No. KRF-2004-005-C00004).

Supporting Information Available: Molecular parameters used in RRKM calculations, such as the harmonic vibrational frequencies and rotational constants; the matrix formulation for simulating the kinetics; thermochemical parameters of activation for all elementary steps. This material is available free of charge via the Internet at http://pubs.acs.org.

References and Notes

(1) Winkler, J.; McLafferty, F. W. *J. Am. Chem. Soc.* **1973**, *95*, 7533.
(2) McLafferty, F. W.; Winkler, J. *J. Am. Chem. Soc.* **1974**, *96*, 5182.
(3) McLafferty, F. W.; Bockhoff, F. M. *J. Am. Chem. Soc.* **1979**, *101*, 1783.
(4) Dunbar, R. C.; Honovich, J. P.; Asamoto, B. *J. Phys. Chem.* **1988**, *92*, 6935.
(5) Baer, T.; Morrow, J. C.; Shao, J. D.; Olesik, S. *J. Am. Chem. Soc.* **1988**, *110*, 5633.
(6) Buschek, J. M.; Ridal, J. J.; Holmes, J. L. *Org. Mass Spectrom.* **1988**, *23*, 543.
(7) Olesik, S.; Baer, T.; Morrow, J. C.; Ridal, J. J.; Buschek, J. M.; Holmes, J. L. *Org. Mass Spectrom.* **1989**, *24*, 1008.
(8) Dunbar, R. C.; Lifshitz, C. *J. Chem. Phys.* **1991**, *94*, 3542.
(9) Lifshitz, C.; Kababia, L. S.; Dunbar, R. C. *J. Phys. Chem.* **1991**, *95*, 1667.
(10) Choe, J. C.; Kim, M. S. *Int. J. Mass Spectrom. Ion Processes* **1991**, *107*, 103.
(11) Lin, C. Y.; Dunbar, R. C. *J. Phys. Chem.* **1994**, *98*, 1369.
(12) Cho, Y. S.; Kim, M. S.; Choe, J. C. *Int. J. Mass Spectrom. Ion Processes* **1995**, *145*, 187.
(13) Shin, S. K.; Han, S. J.; Kim, B. *Int. J. Mass Spectrom. Ion Processes* **1996**, *157/158*, 345.
(14) Kim, B.; Shin, S. K. *J. Chem. Phys.* **1997**, *106*, 1411.
(15) Kim, B.; Shin, S. K. *J. Phys. Chem. A* **2002**, *106*, 9918.
(16) Shin, S. K.; Kim, B.; Jarek, R. L.; Han, S. J. *Bull. Korean Chem. Soc.* **2002**, *23*, 267.
(17) Shin, S. K. *Chem. Phys. Lett.* **1997**, *280*, 260.
(18) Smith, B. J.; Hall, N. E. *Chem. Phys. Lett.* **1997**, *279*, 165.
(19) Kim, S.-J.; Shin, C.-H.; Shin, S. K. *Mol. Phys.* **2007**, *105*, 2541.
(20) Baer, T.; Hase, W. L. *Unimolecular Reaction Dynamics: Theory and Experiments*; Oxford University Press: New York, 1996.
(21) Houston, P. L. *Chemical Kinetics and Reaction Dynamics*; McGraw-Hill: New York, 2001.

JP801098P